Wide frequency range shear modulus dispersion of soft tissue samples measured by magnetic resonance elastography

D. Klatt[1], K. Riek[2], H. Nuzha[1], S. Müller[3], I. Sack[1], and J. Braun[2]
[1]Radiology, Charité - Universitätsmedizin Berlin, Berlin, Berlin, Germany, [2]Medical Informatics, Charité - Universitätsmedizin Berlin, Berlin, Berlin, Germany, [3]Neurology, Charité - Universitätsmedizin Berlin, Berlin, Berlin, Germany

Background: The complex shear modulus G* is sensitive to the micro structural constitution and physiological state of soft biological tissue. MR elastography (MRE) [1] can measure the dispersion of G* in an extended range of frequencies by exploiting either a superposition of multifrequency shear vibrations [2] or by incrementing single drive frequencies in consecutive experiments [3]. In vivo multifrequency MRE has been demonstrated in a frequency range between 25 and 62.5 Hz on human liver [4], brain [5] and skeletal muscle [6]. High field MRE in animal scanners can extend the dynamic range of the measured shear modulus to 1 kHz. This provides important information for modelling the principal viscoelasticity properties of biological tissue in order to obtain i) frequency independent parameters applicable to human MRE at different drive frequencies and ii) insight into micro structural tissue properties which determine the global viscoelastic behavior of biological tissue.
Problem: Only few elastography data have been published on the dynamics of the complex shear modulus in a frequency range of 100 Hz to 1 kHz and a comparison to the low-dynamic range applicable to humans is still vague.
Objective: The study aims to investigate the complex modulus dispersion of tissue samples in a 7T animal MRI scanner. Based on experimental data acquired over a wide dynamic range from 100 to 800 Hz, frequency independent material parameters are deduced by viscoelastic modelling. As model function the springpot element was employed that incorporates two parameters related to the lossless spring constant and the topology of the tissue-inherent micro-structural mechanical matrix. Both parameters are evaluated for samples of gel, brain, muscle, normal liver and fibrotic liver.

Methods fresh bovine liver, bovine muscle and calf brain were obtained from a slaughterhouse immediately before the experiments. A sample of human fibrotic liver (biopsy-proven METAVIR score 3) was obtained from the Clinic of Transplant Surgery and examined within 2 hours after removal. An agarose gel sample was prepared for comparison of biological samples to nondispersive media. A 50 ml Eppendorf tube mounted on a carbon fiver piston with vibration coil was used for fixation of sample position and inducing cylindrical shear waves from the walls to the centre of the tissue sample. In muscle the fibre orientation was parallel to the long axis of the tube. Tissue vibrations of frequencies of f = 100, 200 .. 800 Hz were measured in a transversal view in a 7T scanner (Bruker PharmaScan 70/16, Ettlingen, Germany) by a gradient echo sequence enhanced by sinusoidal motion sensitizing gradients (MEG). Imaging sequence parameters: FoV: 40 mm, slice thickness: 2 mm, 128 x 128 matrix, TR = 114 to 134 ms, TE: 16 ms, MEG direction: through plane (slice selection), MEG amplitude: 285 mT/m, MEG frequency: matched to vibration, number of MEG periods: 1..8 to fit within TE/2. Data were processed by phase unwrapping, temporal Fourier transformation yielding complex wave images $U(x,y,f)$ and direct inversion $(G^*(x,y,f)=-\rho(2\pi f)^2U/\Delta U)$. G^* was spatially averaged in a region of interest given by the boundaries of the sample in the transversal view and fitted by the springpot model function $G^*(\omega)=\kappa(i\omega)^\alpha$ with κ and α as variables. κ is equal to the shear elasticity μ assuming unit viscosity. α is related to the slope of the G^*-dispersion which increases with the degree of freedoms in the micromechanical network. All experiments (aside those of gel and fibrotic liver) were repeated three times on different days and different specimen in order to allow for experimental variations and standard deviations of the derived viscoelasticity parameters.

Results: Figure 1 shows the imaginary part of complex wave images obtained by 600Hz mechanical excitation of samples of liver and muscle tissue. Wavelength and wave damping are represented by storage and loss modulus G' and G". In figure 2 experimental G' and G" data and corresponding fits are shown. In gel, the increase in G' and G" with f is comparably small, while all biological tissue samples show a distinctly higher dispersion of the complex modulus. All samples showed a solid-like material behavior characterized by a G"/G' ratio < 1. The shear modulus μ and the α-parameter (given in brackets) derived by the springpot model were 4.0 kPa (0.17), 7.0±0.2 kPa (0.37±0.01), 4.3±0.7 kPa (0.31±0.01), 56±23 kPa (0.25±0.02), 57.5 kPa (0.34) for agarose, calf brain, bovine liver, bovine muscle and fibrotic liver, respectively. Of note, for comparison of μ to human MRE the specific viscosity of the material has to be accounted for [4,5].

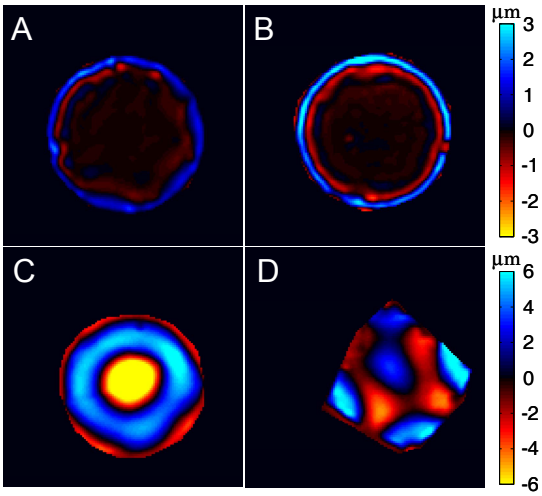

Fig.1: wave images acquired by an excitation frequency of 600 Hz in calf brain (A), bovine liver (B), bovine muscle (C), and human fibrotic (METAVIR score of 3) liver (D).

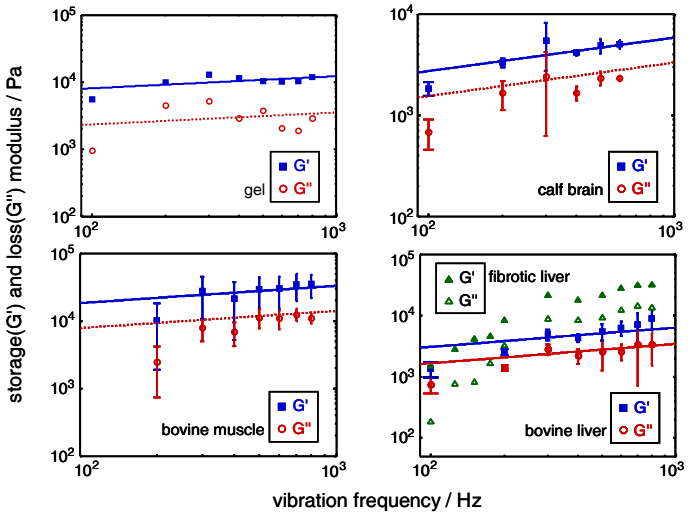

Fig.2:: Experimental data of storage modulus G' (real part of G*) and loss modulus G" (imaginary part of G*). Corresponding springpot-fits are shown by line graphs.

Discussion: Wide-dynamic range MRE data were modeled by a powerlaw simplification of the G*-dispersion for quantifying similarities and principal differences in the architecture of the mechanical matrix of various biological tissue. While healthy liver and brain tissue present a similar viscoelastic behavior, excised muscle appears as stiff and less dispersive material with a lower number of vibrational freedoms (lower value of α) than present in liver or brain (higher value of α). Accounting for the specific viscosity of liver and brain a good agreement was found between wide-dynamic range MRE and in vivo human MRE. A combination of histological proven tissue structure and wide dynamic range MRE may provide the background for in-depth analysis of in vivo human MRE data and the relation between structural changes and disease.

Literature: [1] Muthupillai et al. Science 1995;269:1854-7. [2] Klatt et al. Phys Med Biol 2007;52:7281-94. [3] Klatt et al. Proc ISMRM 2010:632. [4] Asbach et al. Radiology 2010; doi:10.1148/radiol.10092489. [5] Sack et al. Neuroimage 2009;46:652-7. [6] Klatt et al. Phys Med Biol. 2010;55:6445-59.